17th World Conference on Earthquake Engineering, 17WCEE
Sendai, Japan - September 13th to 18th 2020

INITIAL STRESS APPROACH TO HIGH STRENGTH R/C COLUMN AND ITS APPLICATION TO HIGH-RISE BUILDING UNDER SEISMIC LOAD

M. Horikawa[1], K. Asari[2], K. Kuroda[3] and S. Urushihara[4]

[1] *Assistant Professor, College of Engineering, Nihon University, horikawa.masayuki@nihon-u.ac.jp*
[2] *Professor, College of Engineering, Nihon University, asari.kazushige@nihon-u.ac.jp*
[3] *Graduate school, College of Engineering, Nihon University, k.kuroda625@gmail.com*
[4] *Master of Engineering, AUM Structural Engineering Co., LTD, uru@aum.ne.jp*

Abstract

This paper presents a procedure for evaluating the initial stresses induced in the interior column under sustained compressive force and an introduction of those stresses into the multi-spring model enabled to include an interaction between varying bending moments and axial forces at critical sections of column. Then, the lateral cyclic loading test on the high strength R/C column specimen, which has been loaded under the sustained axial force for about three years, was analyzed using the proposed procedure and the caluculated results were compared with the test results to investigate validity of the model. Furthermore, the proposed procedure is applied to full scale R/C building and investigate impacts of initial stresses induced in column on serviceability, design and ultimate limit stage by pushiover analysis.

Keywords: High-rise R/C Building, High Strength Material, Shrinkage, Creep, Multi Spring Model

1. Introduction

The high heat of hydration produces the thermal strain and autogenous shrinkage strain in the high strength concrete. Consequently, these strains cause numerous cracks in the reinforced concrete components due to the confinement effect to reinforcing bars [1]. In addition, the creep strains progress in the columns of lower stories under the high axial forces [2]. Thus, for the seismic response evaluation of the high-rise R/C buildings, it must be indispensable not only to evaluate the elasto-plastic behaviors and time dependency of high strength concrete; that is initial stresses, but also to develop an efficient numerical procesure to integrate those issues in the above. This paper describes the estimation method predicting the initial stresses and the elasto-plastic behavior, and presents the procedure to introduce the initial stresses into the mulit spring model. Then, the proposed system shall be verified with the cyclic lateral loading test available full and detailed experimental information. Furthermore, paying attention to the size dependency of early age behaviors [3], the results of the shaking table test on the scaled R/C building with 20 stories [4] are restored to those of the full-scale building according to the law of similitude. Finally, the incremental loading analysis is carried out, and the effect of the initial stresses in RC columns on the limit state of the full scale RC building with 20 stories is discussed.

2. Numerical Procedure

The whole picture of the system is illustrated in Fig.1. The system is calssified into the followings: 1) the evaluation of initial stresses during the early ages, 2) the evaluation of initial stresses over long-term, and 3) the introduction of initial stresses into the constitutive law and the evaluation of the short term behaviors. The initial stresses during the early ages are caused by constraining free strain induced in the high strength concrete by the reinforcing bar. With reference to the estimation model of the coefficient of linear thermal expansion and the autogenous shrinkage by Teramoto et al. [7] including the effective age obtained from the heat conduction analysis, the estimation model of the dry shrinkage strain and the development of Young's modulus by CEB [8], and the creep model of double law type by Bazant et al. [9], the authors developed the estimation

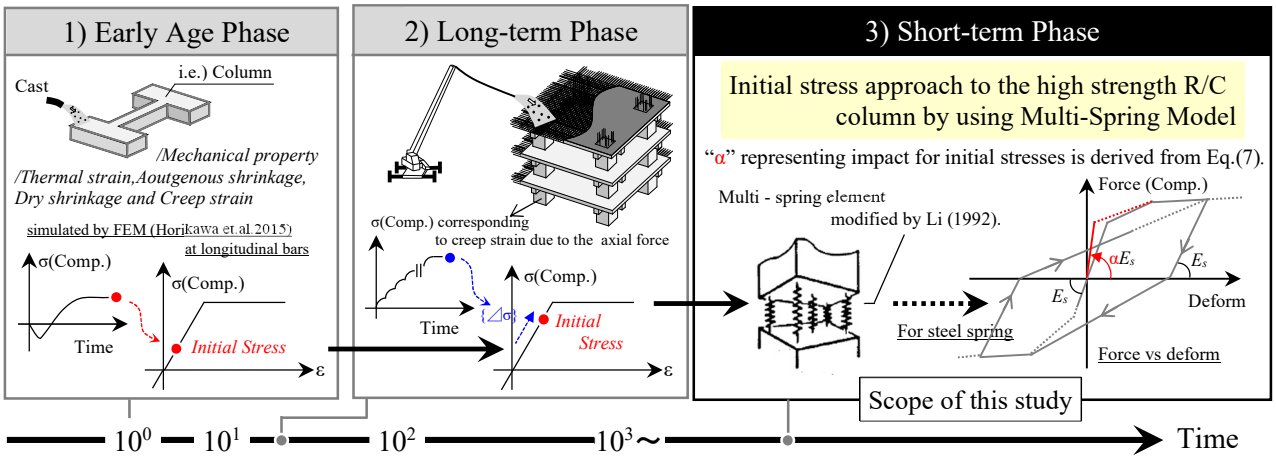

Fig. 1 – Schematic flowchatr for initial stresses approach to inner column

method for predicting the initial stresses in the high strength R/C column. Furthermore, the predicted results by the proposed procedure were compared with the observed ones and the validity of the procedure was verified. In order to predict autogenous shrinkage strain of the ultra high strength concrete, Teramoto et al. presented the following equation in terms of the water binder ratio, the temperature of mixed concrete and the heat history of hydration as:

$$\{\Delta\varepsilon_c\} = \frac{(1-V_a)(K_a/K_p+1)}{1+K_a/K_p+V_a(K_a/K_p-1)}\{\Delta\varepsilon_p(t_e)\} \tag{1}$$

Where, $\{\Delta\varepsilon_c\}$: the incremental strain vector indicating the autogenouse shrinkage strains in concrete, K_a: the bulk modulus of aggregate, K_p: the bulk modulus of cement paste, V_a: the aggregate volume ratio. $\{\Delta\varepsilon_p(t_e)\}$ is the incremental strain vector indicating the autogenouse shrinkage strains in cement paste, and expressed by the following equation as:

$$\{\varepsilon_p(t_e)\} = -\frac{\{\varepsilon_{sh1}\}}{1+e^{(t_e-a)}} - \{\varepsilon_{sh2}\}\cdot exp\left(-\frac{t_e}{1000}\right) + \{\varepsilon_{shmax}\} \tag{2}$$

Where, t_e: the effective age, a: the coefficient to be determined on the temperture of mixed cement paste and the amount of high performance water reducing agent, $\{\varepsilon_{sh1}\}$ and $\{\varepsilon_{sh2}\}$: the autogenous shrinkage strain vector caused during the stage-1 and stage-2, $\{\varepsilon_{shmax}\}$: the maximum autogenous shrinkage strain vector. When the free strain is constrained, the streesses will be induced in the RC element. The creep strain caused by these sustainable stresses can be modeled by the Duble Power Law proposed by Bazant and Osman [9]. The creep compliance can be expressed as follows:

$$J(t,\tau) = \frac{1}{E(\tau)}[1 + q\tau^{-d}(t-\tau)^p] \tag{3}$$

Where, q, d and p are the material constant. For the validity of this method, see the reference [5] and [6]. Since this study aimes to predict the initial stresses during the early ages, the estimation procedure stated in the above shall be adopted. On the other hand, the initial stresses accumulated over the long term are calculated by multiplying the compressive creep strains in concrete induced due to the long-term axial forces by the Young's modulus of reinforcing bars. The creep compliance can be calculated by the following equation as:

$$J(t,t_0) = \frac{1}{E_c(t_0)} + \frac{\emptyset(t,t_0)}{E_{c28}} \quad (4)$$

Where, $J(t,t_0)$: the creep compliance, $E_c(t_0)$: the Young's modulus of concrete under loading, E_{c28}: the Young's modulsu at the age of 28 days, $\emptyset(t,t_0)$: the creep coefficient, t_0: the age of initial loading and t: any age. The introduction of initial stresses shall begin with calculating the axial forces acting on the column section on the basis of the equilibrum condition of forces under the assumption of perfect bond.

$$N_S(t,t_0) = N_{SE} + N_{S-E} + N_{S-L} \quad (5)$$

Where, N_{SE}: the elastic axial force of longitudinal bar transferred through the bond, N_{S-E}: the accumulated axial force of longitudinal bar during the early ages to be evaluated by FEM, and N_{S-L}: the accumulated axial force of longitudinal bar due to the long term creep. $N_S(t,t_0)$ is the axial force in the rebar induced at a certain time and expressed as follows:

$$N_C(t,t_0) = N - N_S(t,t_0) \quad (6)$$

Where, N indicates the applied axial force. Assuming that the axial force is constant, since $N_S(t,t_0)$ increases with time, thus $N_S(t,t_0)$ decreases with time. $N_S(t,t_0)$ corresponds the initial stress to be redistributed due to the time dependency of concrete. Next, the elasto-plastic constitutive law expressing the rebar spring in the multi spring model shall be modified such that Eq.(6) is satisfied. Since this paper takes the compressive creep strain into consideration, only the Young's modulus of compression side shall be modified (Fig.1). In this case, the correction factor, α, is determined by the following equation:

$$\alpha = \frac{1}{E_S}\{N_S(t,t_0)/(\varepsilon_c(t,t_0) \times A_S)\} \quad (7)$$

Where, A_c indicates the cross section of column, E_c: the Young's modulus under loading. $\varepsilon_c(t,t_0)$ means the strain in concrete at acertain time and is calculated by the following equation:

$$\varepsilon_c(t,t_0) = N_C(t,t_0)/(A_C \times E_C) \quad (8)$$

Finally, the elastic anaysis will be carried out after applying the constant axial force to the modified model. It is judged that an introduction of the initial stresses has been completed if the results satisfy Eq.(6). In the evaluation of elasto-plastic behaviors, the multi spring model presented by Lai and Otani and after modified by Li [10] is adopted to take an interaction between the axial forces and the bending moments into consideration. The multi-spring elements consisting of the discretized concrete and steel springs are allocated at the end of member. The force versus displacement relationship is shown in Fig.2.

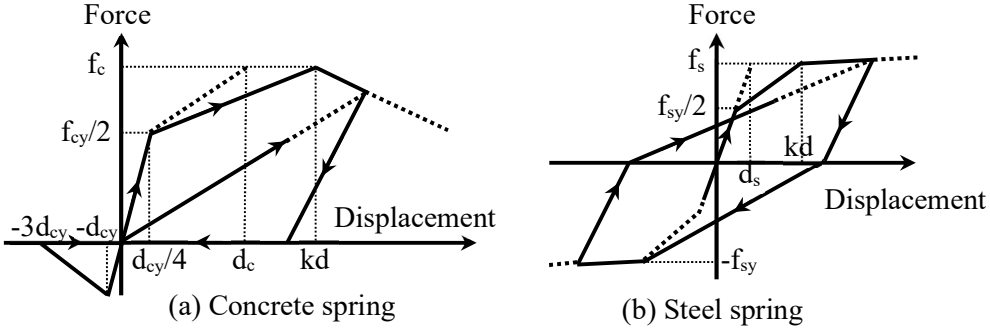

(a) Concrete spring (b) Steel spring

Fig. 2 – Force versus displacement relationship for concrete and steel springs

The force versus displacement relationship of trilinear type for both springs is assumed to include the rotation deformation due to the pullout of tensile rebars from the beam and/or column joint. The stiffness reduction factor of the springs before reaching to the maximum strength is approximated by the following equation:

$$k = 1.0 + \frac{h_0/D - 1}{h_0/D} \tag{9}$$

Where, h_0/D means the shear span ratio of column. The reloading hysteresis path of the steel spring will be oriented to the yielding point to include an effect of the bond slip between concrete and rebar. Even if each concrete spring has different volume, an equal compressive fracture energy is assumed for all concrete springs. In addition, the axial and shear behaviors shall be assumed to be elastic.

3. Verification of Proposed Procedure

For the verification of the proposed model, the R/C column specimen tested in the past [11] will be analyzed. The compressive strength and the tensile splitting strength of concrete at age of 28 days are 150.1(N/mm^2) and 7.33(N/mm^2), respectively. The yield strength of rebar ranges from 720.7(N/mm^2) to 1374(N/mm^2). The geometry and loading setup are shown in Fig.3. The specimen was constructed by horizontally casting concrete, then the specimen covered by sheet was cured under the moisture condition for the age of 7 days, and the formwork was removed from the specimen at the age of 8 days. The strain of concrete or steel and the temperatures in concrete were measured with the strain gauges embedded in concrete or pasted on the surface of reinforcing bars and the thermocouples, respectively. After the age of 28 days, the constant concentric compressive axial force (axial force ratio of 0.3) was sustainably applied on the column for about 1,400 days. Then, after the axial force was once unloaded, the lateral loading test was conducted at the age of 1,443th day.

For evaluating the autogenous shrinkage strain, the parameters were set as follows; $V_a = 0.6$, $a = 17$, $K_a = 39.8$, $K_p = 16.0$. On the other hand, $q = 3.0$, $d = 0.35$ and $p = 0.3$ were assumed for the double power law. The long term creep strains by the sustained axial force were calculated according to the CEB Model Code, and the relative humidity around the ambient environment was assumed to be 60(%). Fig.4(a) compares the simulated results on early age and the long term creep with the test results. The proposed model generally captures the test results. For the detailed verification of early age behaviors, refer to the related papers. The test results are shown in Fig.4(b). Note that the specimen of DHNO.2 was left alone for 1,443 days after casting. Although this specimen is less than the balanced reinforcement ratio, a constant axial force close to the balancing axial force is acting. Thus, it might be judged that the compression failure of concrete preceded and then the yielding of reinforcing bar under compression led to the failure. For this reason, the calculated maximum capacity is well over the test one. After reaching the maximum capacity, the shear crack occurred and it led to the failure of specimen. The effect of this failure mode on the initial stresses is to promote the early yielding of rebars under compression and to enhance the stiffness and capacity slightly, but to deteriorate the ductility.

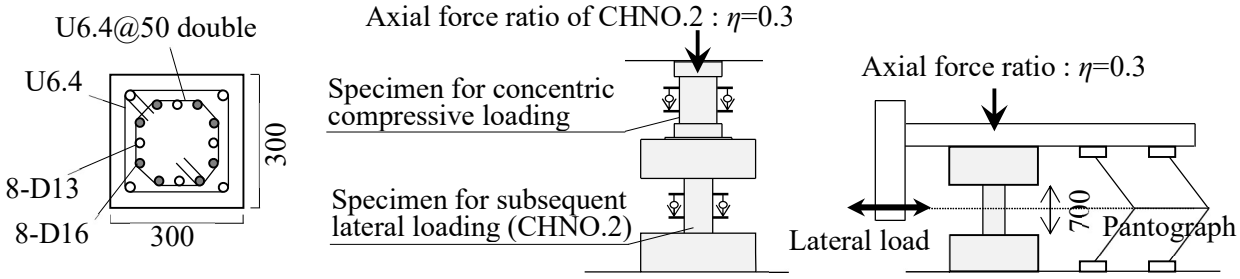

Fig. 3 – (a) is detail of cross section of specimen (mm), (b) is long-term axial loading test, (c) is short-term cyclic loading test (mm).

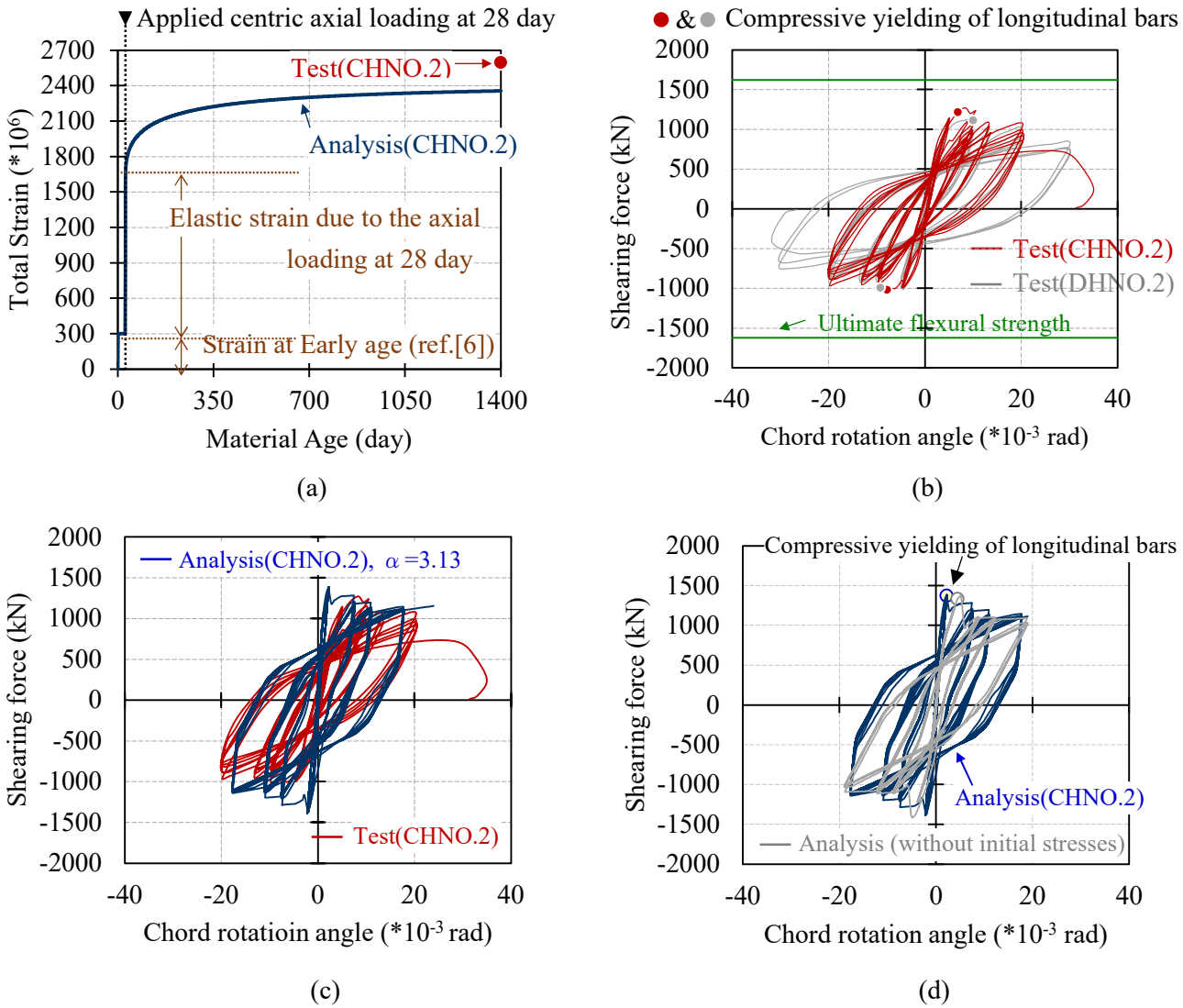

Fig. 4 – (a) Changes in total strain with material ages including early age and long-term behaviors, (b) Test results of shearing force versus chord rotation angle relationship under cyclic loading, (c) Comparison between test and analysis results on CHNO.2, (d) Impact of initial stresses on column failing in shear after flexural compressive yielding.

The calculated elasto-plastic behavior is compared with the test one in Fig. 4(c). The coefficient of k to include the rotation at the joint was assumed to be 1.0 on the basis of parametric study using $k = 1.0 \sim 1.14$. The Komuro model [12] expressing the modified stress versus strain relationship for core concrete originally proposed Muguruma et al. was adopted. The analysis overestimates the initial stiffness and the capacity in each cycle. One of the reasons may be due to the neglect of shear cracks in the cover concrete. Fig.4(d) compares the calculated result without initial stresses with the test result. It is seen that the analysis with initial stresses estimates slightly higher initial stiffness and capacity, and thus it is able to reproduce the early yeilding of rebars under compression. Consequently, as for the column including the early age behaviors and subjected to the sustained concentric axial force, the proposed introduction method of initial stresses can be generally accepted.

4. Application to Full Scale High Rise R/C Building

In this section, in order to apply the proposed model to the full-scale building, the earthquake responses experimentally observed on the scaled R/C building with 20 stories in the E-Defence [4] shall be scaled up to the full-scale responses according to the similitude law. First, it is indispensable to understand the relation among the representative scaling factors. However, it is hard to identify all the scaling factors with reference to the test results reported, and thus the assumed similitude relationship will be verified.

4.1 Similitude Relationship

The scaling factor for the specimen size is 1/4. For the dynamic problem, it is common to assume the scaling factor for the gravitational acceleration to be 1.0. In addition, if the scaling factor for the mass density is set to be 1.0, the following relationship for the scaling factor S can be derived as [13]:

$$S_a \cdot S_\rho \cdot S_l = S_\sigma \tag{10}$$

Where, the subscripts a, ρ, l, and σ indicate the acceleration, the mass density, the size and the stress, respectively. For the dynamic problem, earch scaling factor can be optionally so determined to satisfy Eq. (10). Now, if the scaling factors for S_σ and S_a are set to be 1.0, the ideal factors listed on the upper rows in Table 1 may be derived. However, the specimen tested on the shaking table considered used the same material as to one of the prototype one, and thus, S_ρ also becomes 1.0. Since S_l = 1/4, there scaling factors could not satisfy the condition of Eq. (10). Consequently, it is envisaged that the additional weights were added on the model specimen to cmpensate this inconsistency. The similitude relationship for the weight can be expressed by the following equation as:

$$W_m = (S_\rho \cdot S_l^3 \cdot S_a) W_p \tag{11}$$

For determining the weight of the test model, substituting $S_\rho = S_a$ = 1.0 and S_l = 1/4 into Eq. (11), then $W_m = 1/4^3 W_p$ can be derived. This means that the weight of the target experiment is 1/4 times one of the ideal scaling case (Table 1 upper row).

The scaled-up dimensions of the full-scale building are listed in Table 2. The spacing of hoops does not satisfy the current deisgn criteria when S_l = 1/4 is applied. In this paper, the ultimate shear strengths for columns and beams were determined to satisfy the similitude relationship, thus leading to the scaling factor of 1.0 for the shear reinforcement ratio p_w. Accordingly, it is able to so assign any values for the area and spacing of shear reinforcing bars to satisfy the condition. For example, the ultimate shear strength of beams could be calculated by the following equation:

$$Q_u = \left\{ \frac{0.068 {p_t}^{0.23} \cdot (f_c + 18)}{\left(\frac{M}{Q \cdot d}\right) + 0.12} + 0.85\sqrt{p_w \cdot \sigma_{wy}} \right\} \cdot b \cdot j \tag{12}$$

$$p_w = a_w / (b \cdot x) \tag{13}$$

Where, p_t: the tensile steel ratio, f_c: the compressive strength of concrete, M/Q: the shear span ratio, d: the effect depth, p_w: the shear reinforcement ratio, σ_{wy}: the yielding strength of shear reinforcement, b: the width of members, j: the lever arm, a_w: the area of one set of shear reinforcement, x: the spacing of shear reinforcing bars.

Table 1 – Assumption of scaling factor and ideal scaling in the test

Dimension	Force	Acceleration	Velocity	Time	Length
Scaling Factor of True replica	$1/4^2$	1	1/2	1/2	1/4
Assumption of Scaling Factor	$1/4^2$	1	1/2	1/2	1/4
Dimension	Modulus	Stress	Strain	Mass density	Weight
Scaling Factor of True replica	1	1	1	4	$1/4^2$ (≈ 0.06)
Assumption of Scaling Factor	1	1	1	1	$1/4^3$ *

*The model specimen has an additonal weight of 125(kN)*20(floor) = 2500(kN), according to the ref.[4]

Table 2 – Specification of full-scale building assumed by authors on the basis of reference [4]

Floor	Column 900×900(mm)				Floor	Beam 600×800(mm)	
	C22	C12	C11	C21		GX	GY
20～17	8-D38 #-D13@90, p_t=0.42, p_w=0.63				R,20	3/3-D38 2-D13@100 p_t=0.82, p_w=0.42	3/3-D38,2-D13@100 p_t=0.90, p_w=0.42
17～13	8-D38 #-D13@90, p_t=0.42, p_w=0.63			12-D38 #-D13@90, p_t=0.56, p_w=0.63	19,18	3+1/3-D38 2-D13@100 p_t=0.82, p_w=0.42	3+1/3-D38,2-D13@100 p_t=0.90, p_w=0.42
13～8	8-D38 #-D13@90 p_t=0.42, p_w=0.63	12-D38 #-D13@90 p_t=0.56, p_w=0.63	8+1-D51 #-D13@90 p_t=0.75, p_w=0.63	12-D38 #-D13@90 p_t=0.56, p_w=0.63	17,16	3+1/3-D38 2-D13@85 p_t=0.82, p_w=0.50	3+2/3+1-D38,2-D13@85 p_t=1.27, p_w=0.50
8～2	12-D38 #-D13@90 p_t=0.56, p_w=0.63	12-D51 #-D13@90 p_t=1.00, p_w=0.63	12+2-D51 #-D13@90 p_t=1.00, p_w=0.63	12-D51 #-D13@90 p_t=1.00, p_w=0.63	15～13	3+2/3+1-D38 2-D13@85 p_t=1.16, p_w=0.50	3+2/3+2-D38,2-D13@85 p_t=1.65, p_w=0.50
					12～9	3+2/3+1-D38 2-D13@60 p_t=1.16, p_w=0.70	3+2/3+2-D38,2-D13@60 p_t=1.65, p_w=0.70
1	12-D38 #-D13@50 p_t=0.56, p_w=1.13	12-D51 #-D13@50 p_t=1.00, p_w=1.13	12+2-D51 #-D13@50 p_t=1.00, p_w=1.13	12-D51 #-D13@50 p_t=1.00, p_w=1.13	8～2	3+3/3+2-D38 2-D13@60 p_t=1.50, p_w=0.70	3+3/3+3-D38,2-D13@60 p_t=2.03, p_w=0.70

4.2 Verifications of Similitude Relationship

The total wieght of the full-scale building shown Table 2 excluding the weight of foundation was caluculated as 68,617 (kN). According to the paper [4], the weight of model specimen with the additional weight but excluding the weight of foundation was reported as 3,557 (kN). Thus, the scaling factor of the weight becomes 0.05, and this factor roughly coincides with the ideal scaling factor of the weight shown in Table 1.

The modeling of columns was similar to that in the section 2, but the confinement effect of the core concrete was included by applying the method by Mander [14]. The Takeda model [15] was applied to model the restoring force characteristics of beams. The beam-column joints and slabs were assumed to be the rigid body. The pushover analysis was carried out by incrementally applying the lateral forces of the Ai distribution to the model specimen. The test responses in Fig.5 indicate the modified ones by multiplying the maximum responses of the shaking table test by the scaling factor. Note that shaking table test was conducted with the five different long-period seismic motions. The numerical results clearly confirm the validity of the analysis model and similitude law. The formation of the plastic hinges at the ends of beams over the height suggests the total collapse mechanism just like the test result.

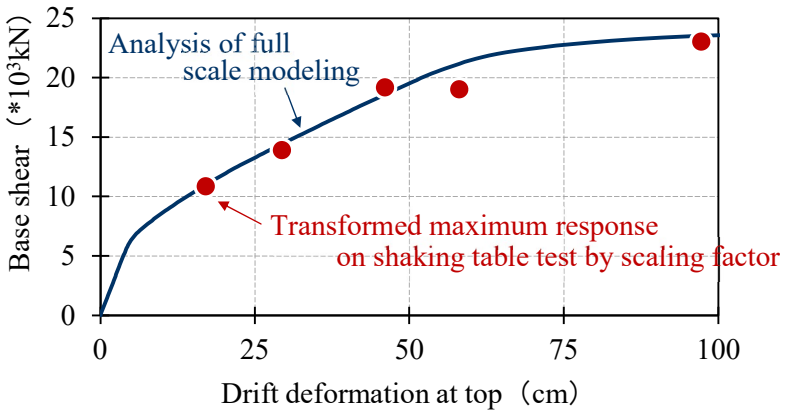

Fig. 5 – Predicted base shear versus drift deformation at top

4.3 Impact of Initial Stresses in Column on Elasto-Plastic Behavior of R/C Building

Fig.6 shows the change in the axial forces of rebar in inner column of the first story bearing the sustained concentric compressive axial force. The axial forces of the vertical axis are calculated by Eq. (5). Note that N_{S-E} in Eq. (5) was assumed to be 80 (N/mm^2) per one rebar on the basis of the finite element stress and creep analysis presented by the authors. The axial force was applied to the first story at the age of 28 days, and the weight of each story was applied every 28 days by a step-by-step mannner. The duration of sustained axial loading shall be up to the age of 3,000 days at which the change of axial force settle down a certain value. As a result, the axial force of 1,036 (kN) is acting at the age of 3,000 days. Also, the elastic analysis was carried out under the same condition, and the axial force acting in the rebar was 548 (kN). Since the total axia force acting on the inner column of first story was 6,810 (kN), the fraction of the axial force bone by the rebar increased from 8% to 15%. Fig.7 shows the results by the pushover analysis in the lateral direction. The limit states prescribed in "Design guideline based on inelastic displacement (AIJ, 1999)" [16] are also plotted in the figure. The story shear force versus story drift relationship for 1-st and 8-th story is almost similar to each other, and the effect of initial stresses are minor. However, the story drift at the 20-th story is largely progressing. This may be due to the advancement of the rebar yielding in the ege region of column section at the lower stories which is developed by the initial stresses existing in the R/C column (Fig.8(a)). Fig.8(b) shows the results calculated by applying the lateral forces to the model in the 45 degree direction. It is seen from the figure that the lateral displacements in the Y-direction advance if the initial stresses are included. This

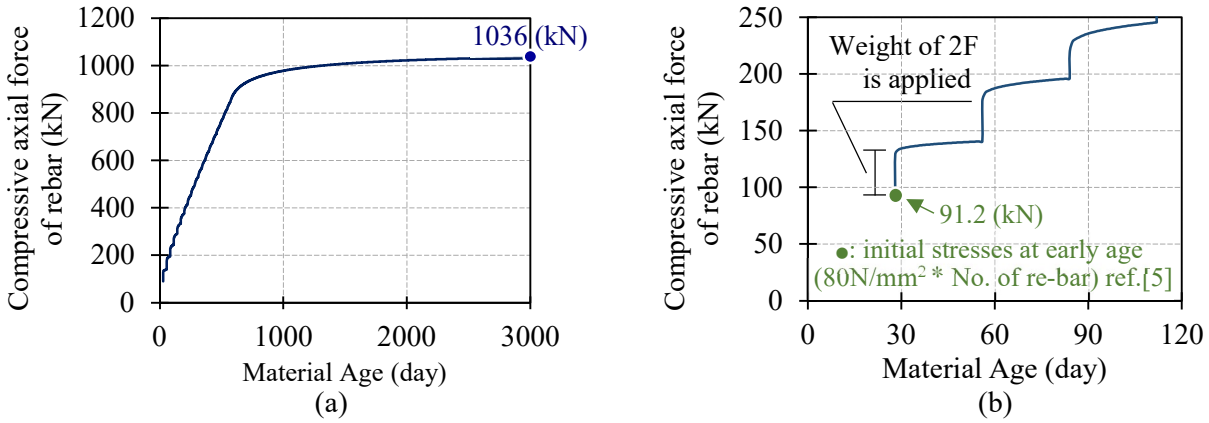

Fig. 6 – (a) Changes in axial force of rebar in inner column at first story with material age, and (b) Changes in axial force of rebar up to material age of 120 dyas.

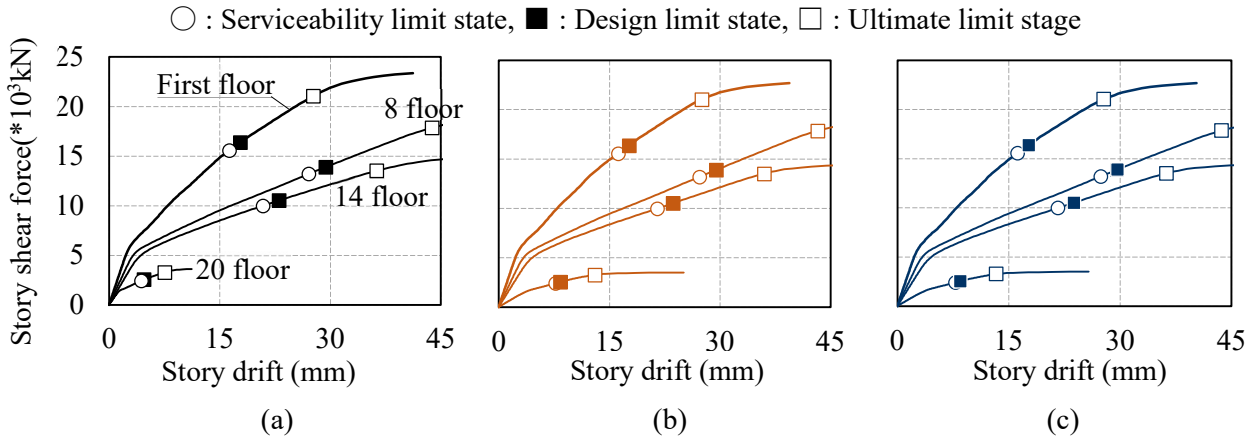

Fig. 7 – Story shear force versus story drift relationships at 1-st, 8-th, 14-th and 20-th floors: (a) without early age and long-term behaviors, (b) with long-term behaviors, (c) with early age and long-term behaviors.

suggests that the initial stresses might influence on the torsional deformation of the building as is seen from the yielding distribution of rebars shown in Fig.8(a).

5. Conclusion

The following results were obtained through the numerical investigation on the R/C inner column and the high-rise R/C building with the proposed model.

(1) The proposed model is generally able to reproduce the elasto-plastic behaviors of the inner column including the initial stresses.
(2) The initial stresses in the R/C Columns promotes the early yielding of rebars in the columns in the lower stories and exerts influences on the deformation in the upper stories.
(3) It may be concluded through the diagonal lateral loading that the initial stresses influence on the torsional deformation of buildings.

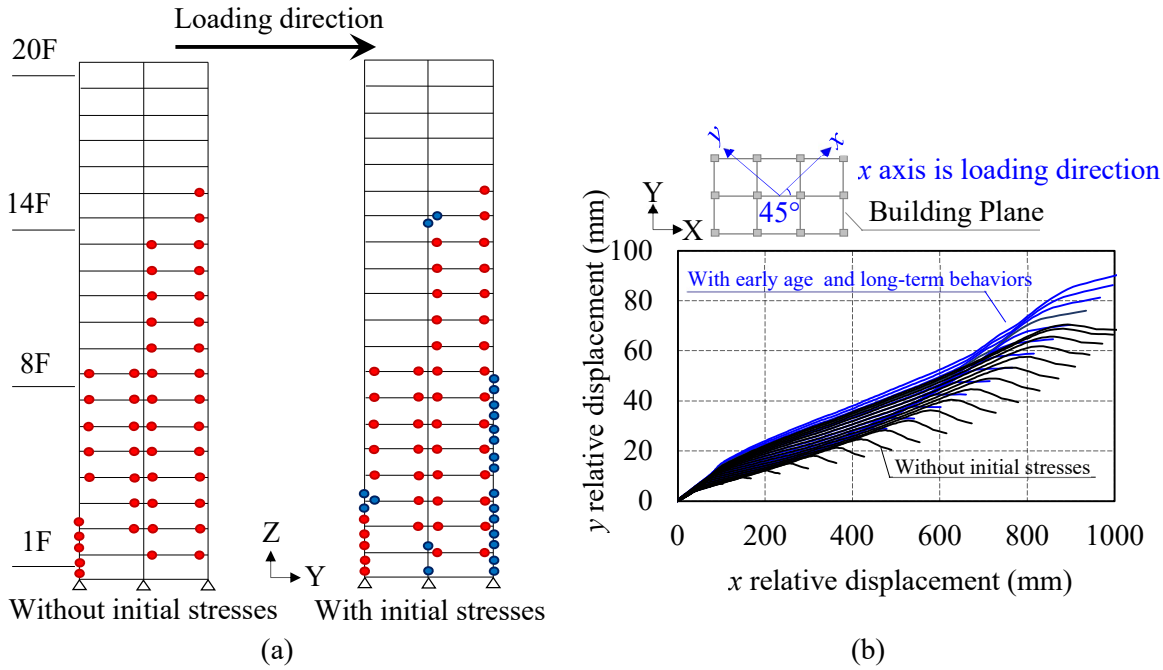

Fig. 8 – (a): Distribution of yielding steel springs, and (b) Displacement in *x* direction relative to ground level against displacement in *y* direction relationship.

6. Acknowledgements

This work was supported by JSPS KAKENHI, Grant-in-Aid for Young Scientists (B), Grant Number JP 17K14763. The authors appreciate Professor Emeritus Nobuaki Shirai of Nihon University, Tokyo, Japan for valuable advices.

7. References

[1] Ippei Maruyama, Masahiro Suzuki, Hirokazu Nakase and Ryoichi Sato (2008): Self-Induced Stress and Resultant Cracks in Reinforced Ultra High-Strength Concrete Column – part 1 Experimental study on the effect of temperature history, J. Struct. Constr. Eng., AIJ, vol.73, No.629, 1035-1042. (in Japanese)

[2] A working group of the concrete centre and fib task group 1.6 (2014): Tall building, 106-123.

[3] Norichika Katayose, Naoki Takamori, Hirokazu Nishida and Masaru Teraoka (2006): Mechanical Property and Autogenous Shrinkage on High-Strength Concrete During Early Age, *Proceedings of JCI*, Vol.28, No.1, 497-502. (in Japanese)

[4] Kuniyoshi Sugimoto, Hideo Katsumata, Hiroshi Fukuyama, Taiki Saito and Toshikazu Kabeyasawa (2012): Earthquake Resistant Performance of High-Rise Reinforced Concrete Buildings under Long-Period Ground Motions, *Proceedings of 15th WCEE*.

[5] Masayuki Horikawa, Tatsunori Shindo, Kazuki Tajima and Nobuaki Shirai (2015): Stress Analysis of High Strength R/C Column Including Early Age Behavior by 3-D FEM, J. Struct. Constr. Eng., AIJ, vol.80, No.715, 1447-1457. (in Japanese)

[6] Masayuki Horikawa and Nobuaki Shirai (2016): Evaluation of Early Age, Long- and Short-term Behavior of R/C Column Including Shrinkage and Creep Effect by 3-D FE Analysis, *Proceedings of 11th fib International PhD Symposium in Civil Engineering*, 849-856.

[7] Atushi Teramoto, Ippei Maruyama, Makoto Tanimura and Yuji Mitani (2010): A Proposal of Prediction Model for Autogenous Shrinkage of Ultra High-Strength Concrete, J. Struct. Constr. Eng., AIJ, vol.75, No.654, 1421-1430. (in Japanese)

[8] Comite Euro-International du Beton (1991): CEB-FIP Model Code 1990, Final Draft, Chapters 1-3.

[9] Bažant, Z.P., Osman, E (1976): Double Power Law For Basic Creep of Concrete, Mat. Constr. **9**, 3-11.

[10] Kang-ning Li (1992): Nonlinear Earthquake Response of R/C Space Frame With Triaxial Interaction, *Proceedings of 10th WCEE*, ISBN 90 5410 060 5.

[11] Yukihiro Satoh, Naoki Takamori, Hitoshi Sasaki, Masashi Matsudo and Masaru Teraoka (2009): Influence of Long-Term Compressive Properties on Seismic Performance of R/C Column Using Ultra-High Strength Materials, Summaries of Technical Papers of Annual Meeting, AIJ, Structures IV. 233-238. (in Japanese)

[12] Tsutomu Komuro, Kazumasa Imai, Akitsugu Muramatsu, Takeyoshi Korenaga and Fumio Watanabe (2004): Compresive Properties of Reinforced Concrete Columns Using High Strength Concrete with Compressive Strength of 100-180 N/mm^2, J. Struct. Constr. Eng., AIJ, No.577, 77-84. (in Japanese)

[13] Harry G. Harris and Gajanan M. Sabnis (1999): Structural Modeling and Experimental Techniques, second edition, CRC Press, 76-77.

[14] J. B. Mander, M. J. N. Priestley and R. Park (1988): Theoretical Stress‐Strain Model for Confined Concrete, Journal of Structural Engineering, ASCE, Vol.114, Issue 8, 1804-1826.

[15] Toshikazu Takeda, Mete A. Sozen, N. Norby Nielsen (1970): Reinforced Concrete Response to Simulated Earthquakes, Journal of the Structural Division, Vol. 96, Issue 12, 2557-2573.

[16] Architectural Institute of Japan (1999): Design Guidelines for Earthquake Resistant Reinforced Concrete Buildings Based on Inelastic Displacement Concept, 426-433. (in Japanese)

